Theory of interactions and phase transitions of hydrogen in transition metals

V. G. Vaks, N. E. Zeĭn, V. I. Zinenko, and V. G. Orlov

I. V. Kurchatov Institute of Atomic Energy, Moscow
(Submitted 13 April 1984)
Zh. Eksp. Teor. Fiz. **87**, 2030–2046 (December 1984)

Analytic methods based on the cluster approximation are proposed for calculating the thermodynamic properties and phase diagrams of hydrogen (H) in transition metals (Me). These methods differ from the mean-field approximation in that they can quantitatively incorporate the blocking and strong oscillatory interactions which are typical of hydrogen in transition metals. Calculations are carried out on the stress-induced and screened Coulomb H–H interactions for the NbH_x and PdH_x systems. The calculations show, in particular, that the blocking seems to be due to an anharmonicity of the stress-induced interactions at short distances between the protons. These new methods are used for calculations on gas-liquid phase transitions of hydrogen in NbH_x and PdH_x. The results indicate that a nonbinary repulsion of protons is important when x is not small.

1. INTRODUCTION

The properties and phase transitions of hydrogen (H) in transition metals (Me) have attracted considerable interest (see Refs. 1–3, for example) because of the promising applications of Me-H systems. These systems are also of general physical interest since they rank among the closest realizations of the lattice-gas model which is widely discussed in statistical physics.[4,5] One of the most urgent problems in the physics of H in Me is to determine the nature of the proton–proton interactions, V_{HH}. These questions are of both fundamental and practical interest, e.g., in connection with the problems of the limiting solubility of H in Me. In bcc transition metals, for example, one observes that a proton will block the neighboring interstitial positions in the first few coordination spheres (it will prevent other protons from assuming positions there); the nature of this blocking is not clear and is the subject of some debate.[1,6]

The temperature-concentration (T-x) phase diagrams of H in Me are usually extremely complicated and show several phase transitions, both gas–liquid transitions and transitions to ordered structures of H in Me (Refs. 1, 2, 7, and 8). Experimental information on these phase transitions might yield much information about the H–H interactions. Theoretically, on the other hand, it is difficult to study these phase transitions, because it is necessary to consider the strong correlations in the positions of the H (including the blocking effect) and the rapidly oscillatory behavior of V_{HH} as a function of the distances R_{HH} which seem to be characteristic of H in Me (Refs. 6 and 9–11). For example, the standard mean-field approximation, which ignores these effects, overestimates the temperatures and concentrations (T_c and x_c) at which the phase transitions occur for H in bcc metals by nearly an order of magnitude (See Ref. 12 and the discussion below). So far, the only quantitative estimates of $T_c(x)$ which have been found for H in Me (in simplified interaction models) have been found by Monte Carlo methods.[6,9–11] These methods, however, require a great deal of computer time, are afflicted by errors which are difficult to estimate, and are poorly suited for (among other questions) extensive studies of the sensitivity of the results to variations in the models.

In the present paper we propose some analytic methods based on the cluster approximation[13–15] for calculating the statistical properties of H in Me. The cluster approximation can deal adequately with these strong correlations and oscillatory interactions. It has proved successful in describing several structural phase transitions, in particular, in crystals with H bonds, which are also characterized by strong correlations in the positions of neighboring protons (the "ice rule").[15] For simple models this method is equivalent to the Bethe-Peierls and quasichemical approximations,[4] but in the form in which it was used in Refs. 13–15 it can also be generalized easily to the cases of strong alternating-sign and long-range forces, nonbinary interactions, complicated real lattices, etc. The accuracy of the method improves as the short-range "intracluster" correlations become stronger. The results found by this method for systems with the ice rule, for example, ususally either coincide with the exact results or are extremely close to them.[15] In Secs. 2, 3, and 5 below we show that this approximation is also highly accurate for realistic models of H in Me and can be used for quantitative estimates of the properties of H in Me in a wide variety of models.

In Sec. 4 we also discuss the available models for the interactions of H in Me. The total interaction V_{HH} in these systems is by convention treated as the sum of a stress-induced term V_{si} and a screened Coulomb ("electronic") interaction V_e (Refs. 6, 9, and 10). The component V_{si} is calculated from data on the phonon spectra and the concentration dependence of spontaneous strains in hydrides.[6,9,12] However, the applicability of the approximations which have been used here (ignoring anharmonic and nonbinary forces, considering the Me–H interactions in only one or two coordination spheres, etc.) is not completely clear and is in dispute.[16,17] The V_e interaction has been calculated in the models of linear[9] and nonlinear screening,[17,18] and the results show a large scatter. We have carried out detailed calculations of $V_e(R)$ in a linear-screening model, using a variety of (the most reliable) approximations for the dielectric function $\varepsilon(q)$, and also varying the effective density of the screening electrons over a broad range. By comparing the results with calculations for a nonlinearly screened V_e (Ref.

 0038-5646/84/121171-11$04.00

18) and with estimates of the band structure of Me-H systems[19] we can draw several conclusions about the nature of V_e. We will show in particular that, in contradiction of the suggestions in Refs. 6 and 10, the $V_e(R)$ component could hardly explain the observed blocking effect. The blocking is more probably due to a pronounced stress-induced anharmonicity at small values of $R = R_{HH}$ and the inapplicability in this case of the ordinary harmonic approximation for V_{si}. We will also show that the component V_e is apparently considerably less important than V_{si} in bcc hydrides of the NbH_x type, while in fcc hydrides of the PdH_x type the V_e and V_{si} components are comparable; in this latter case the total interaction V_{HH} is far less sensitive to the form of V_e than in the bcc hydrides.

In Sec. 5 we use these new methods to describe a gas-liquid phase transition for H in the best-studied systems, NbH_x and PdH_x. Comparing the results with experiment, we draw several conclusions regarding the roles played by various factors in the thermodynamics of H in Me. In particular, we find indications that nonbinary or concentration-dependent forces between protons are important at $x \gtrsim 0.3$–0.5. In the Conclusion we discuss the basic results and some further applications of these new methods.

2. USE OF THE CLUSTER APPROXIMATION IN DESCRIBING HYDROGEN IN METALS

We will be discussing only the "configurational" contributions to the thermodynamics of H in Me—those which depend on the mutual positions of the protons and stem from the H–H interaction. Other contributions, stemming from changes in the band structure, phonon contributions, etc., have been discussed elsewhere (see, for example, Refs. 8, 16, or 2, Vol. 2, Ch. 3). We use the model of a lattice gas,[6,8–12] assuming that the protons occupy positions (pores) of only one type in the lattice, e.g., tetrahedral positions as in NbH_x or octahedral positions as in PdH_x (Ref. 2). The Hamiltonian of the grand canonical distribution, $H' = H - \mu N$, can then be written

$$H' = \sum_{i<j} V_{ij}\hat{n}_i\hat{n}_j - \mu\sum_i \hat{n}_i + \sum_{i<j<k} U_3^{ijk}\hat{n}_i\hat{n}_j\hat{n}_k + \sum_{i<j<k<l} U_4^{ijkl}\hat{n}_i\hat{n}_j\hat{n}_k\hat{n}_l. \tag{1}$$

The operator $\hat{n}_i$ here, which has the value of 0 or 1, describes the filling of pore i by a proton; $\mu = \mu_H$ is the effective chemical potential of hydrogen; and the terms with U_3 and U_4 correspond to a possible contribution of many-particle interactions. The average filling of a pore, $\langle \hat{n}_i \rangle = c$, in the hydride MeH_x (in the absence of an ordering of protons) is proportional to the concentration x. For a tetrapore in a bcc hydride, for example (Fig. 1), we would have $c = x/6$, while for an octopore in an fcc hydride we would have $c = x$. The thermodynamic potential per pore, Ω, and its relation with c are

$$\Omega = -\frac{1}{N_p} T \ln \mathrm{Sp} \exp(-\beta H'), \qquad c = -\left(\frac{\partial \Omega}{\partial \mu}\right)_T, \tag{2}$$

where N_p is the total number of pores in the lattice, $\beta = 1/T$, and the Sp means the sum over all sets of values $\{n_i\}$. We will express Ω and μ as functions of c and T. These configurational contributions to the entropy (s_H) and the enthalpy (h_H) per proton are then given by

$$s_H = -\frac{1}{c}\left(\frac{\partial F}{\partial T}\right)_c, \qquad F = \Omega + \mu c, \qquad h_H = \mu + T s_H. \tag{3}$$

In the case of a gas–liquid phase equilibrium, given values of Ω and μ correspond to two concentrations, c_1 and c_2, determined by

$$\Omega(c_1, T) = \Omega(c_2, T), \qquad \mu(c_1, T) = \mu(c_2, T). \tag{4}$$

The equation for the spinodal (the curve describing the loss of stability with respect to stratification), $T_s(c)$, is of the form $\partial\mu/\partial c = 0$, and the position of the critical point (T_c, c_c) is determined from the system of equations[20]

$$\partial\mu/\partial c = 0, \qquad \partial^2\mu/\partial c^2 = 0. \tag{5}$$

As we will be discussing below, the many constants V_{ij} in (1) are not small in comparison with T near a phase transition of H in Me. For example, the blocking in the first three coordination spheres of H in a bcc metal implies the relation $V_{ij} \gg T$ here. We know that the mean-field approximation breaks down here, but the cluster approximation proves extremely good.[13–15] In this method, groups of several pores, i.e., clusters, are chosen in the lattice, and the thermodynamic average of (1) per pore is written as

$$\varepsilon' = \frac{1}{N_p}\langle H' \rangle = \sum_k \lambda_k \langle H_k' \rangle. \tag{6}$$

Here H_k' is the Hamiltonian of the k th cluster, and the λ_k

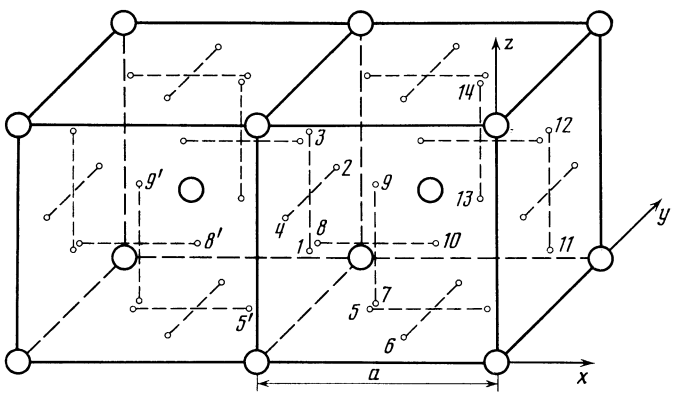

FIG. 1. Tetrahedral interstitial positions (pores) in a bcc metal. Small circles—Pores; large circles—metal atoms; light (dashed) lines—V_2 bonds, shown for clarity.

are numerical constants determined by the lattice geometry and the particular choice of clusters. Here we have the following normalization condition on ε' per pore:

$$\sum_k \lambda_k \nu_k = 1, \tag{7}$$

where ν_k is the number of pores in the k th cluster.

In the cluster Hamiltonian H_k', the interactions within a cluster are described exactly, i.e., just as they are in the original Hamiltonian (1), while the interaction with the surroundings is described approximately by means of variational parameters: the effective fields $\psi_k^{(i)}$. For binary interactions [i.e., for $U_3 = U_4 = 0$ in (1)], for example, the cluster Hamiltonian H_k' and its density matrix $\hat{\rho}_k$ are approximated by

$$H_k' = \sum_{i<j}^{\nu_k} V_{ij}\hat{n}_i\hat{n}_j + \sum_{i=1}^{\nu_k} (\psi_k^{(i)} - \mu)\hat{n}_i, \tag{8a}$$

$$\hat{\rho}_k = \exp(\beta\Omega_k - \beta H_k'), \quad \beta\Omega_k = -\ln Z_k = -\ln \mathrm{Sp} \exp(-\beta H_k'). \tag{8b}$$

Certain relations among the values of $\psi_k^{(i)}$ in different clusters, which make it possible to cancel out terms with $\psi_k^{(i)}$ in sum (6), are established from physical considerations regarding the additivity of the contributions to the field $\psi_k^{(i)}$ at the ith pore from the various pores of the surroundings, i.e., from the various "bonds" in the lattice or from groups of such bonds (see Refs. 13–15 and the discussion below). The values of $\psi_k^{(i)}$ in each of the clusters are determined from matching conditions: the equality of all the averages $\langle \hat{n}_i \rangle$ of the concentration c,

$$c = \langle \hat{n}_i \rangle = -\frac{\partial(\beta\Omega_k)}{\partial \psi_k^{(i)}} = y_k^{(i)} \frac{\partial}{\partial y_k^{(i)}} \ln Z_k, \tag{9}$$

where $Y_k^{(i)} = \exp(\beta\mu - \beta\psi_k^{(i)})$ is the "activity" of a pore, which appears in the expression for Z_k.

Integrating the equation $\varepsilon' = \partial(\beta\Omega)/\partial\beta$, we find from (6)–(9)

$$\Omega = \sum_k \lambda_k \Omega_k. \tag{10}$$

Matching conditions (9) along with the relationships between the fields $\psi_k^{(i)}$ in different clusters are equivalent to the conditions minimizing expression (10) with respect to a variation of $\psi_k^{(i)}$: $\partial\Omega/\psi_k^{(i)} = 0$.

An expression for μ corresponding to (10) can be derived from the thermodynamic relation

$$\frac{\partial\mu}{\partial c} = -\frac{1}{c}\frac{\partial\Omega}{\partial c}. \tag{11}$$

Substituting (10) in here, and integrating over c, using (9), we find

$$\beta\mu = \sum_k \lambda_k \sum_i \ln y_k^{(i)} = \sum_k \lambda_k \nu_k \ln \bar{y}_k, \tag{12}$$

where $\bar{Y}_k$ is the geometric mean of the values of $Y_k^{(i)}$ in a cluster. For "symmetric" clusters, in which all the pores are geometrically equivalent, the values of $Y_k^{(i)}$ do not depend on i, and the sign indicating the average can be omitted from $\bar{Y}_k$ in (12).

As the cluster size ν_k increases, the accuracy of this method obviously improves, but the calculations become more complicated. In practice, the clusters are chosen in such a manner that they include as many as possible of the bonds corresponding to the strongest interactions (see Refs. 13–15 and the discussion below).

To illustrate the method we first consider the simple example of binary clusters, setting $U_3 = U_4 = 0$ in (1). We denote by V_r the interaction V_{ij} in (1) for the rth coordination sphere, and we number a cluster of two pores connected by this "bond" by the index $k = (2, r)$. Relations (6) and (8a) then become

$$\varepsilon' = \langle H_1' \rangle + \frac{1}{2}\sum_{r=1}^{\infty} m_r(\langle H_{2,r}' \rangle - 2\langle H_1' \rangle), \tag{13a}$$

$$H_1' = \hat{n}_0(\psi_1 - \mu), \quad H_{2,r}' = V_r\hat{n}_0\hat{n}_r + (\hat{n}_0 + \hat{n}_r)(\psi_{2,r} - \mu), \tag{13b}$$

$$\psi_{2,r} = \psi_1 - \varphi_r, \quad \psi_1 = \sum_{r=1}^{\infty} m_r\varphi_r. \tag{13c}$$

Here m_r is the coordination number in the rth sphere, φ_r represents the field acting on a given pore along the rth bond, and ψ_1 is the total field at one pore. Introducing $y_1 = \exp(\beta\mu - \beta\psi_1)$, $y_{2,r} = y_1 \exp(\beta\varphi_r)$, we find the following expressions for Ω_1 and $\Omega_{2,r}$, using (8a):

$$\beta\Omega_1 = -\ln(1 + y_1), \quad \beta\Omega_{2,r} = -\ln[1 + 2y_{2,r} + y_{2,r}^2 \exp(-\beta V_r)]. \tag{14}$$

Finally, from (10) and (12) we find

$$\Omega = \Omega_1 + \frac{1}{2}\sum_{r=1}^{\infty} m_r\tilde{\Omega}_{2,r}, \quad \mu = \mu_1 + \sum_{r=1}^{\infty} m_r\tilde{\mu}_{2,r}. \tag{15}$$

Here Ω_1, μ_1 and $\tilde{\Omega}_{2,r}$, $\tilde{\mu}_{2,r}$, are given by the following expressions, where we are using (9) and (12)–(14):

$$\beta\Omega_1 = \ln(1-c), \quad \beta\mu_1 = \ln[c/(1-c)], \tag{16a}$$

$$\beta\tilde{\Omega}_{2,r} = \beta(\Omega_{2,r} - 2\Omega_1) = -\ln\left[1 + \frac{(1 + 4c(1-c)f_r)^{1/2} - 1 - 2cf_r}{2(1+f_r)}\right], \tag{16b}$$

$$\beta\tilde{\mu}_{2,r} = \beta(\mu_{2,r} - \mu_1) = \ln\left[1 + \frac{(1 + 4c(1-c)f_r)^{1/2} - 1 - 2cf_r}{2c(1+f_r)}\right], \tag{16c}$$

where $f_r = \exp(-\beta V_r) - 1$. We see that the interaction effects are described by a Mayer function f_r here instead of by the parameter βV_r, which would be characteristic of the mean-field approximation. For the values of βV_r under consideration here (i.e., values which are not small), this circumstance makes the description much more accurate than the mean-field approximation, while at small values of βV_r expressions (15) and (16) become the expressions of the mean-field approximation.

To take into account the nonbinary, many-particle, correlations, we should consider clusters of large numbers of pores, $\nu > 2$ (which we will call "ν-clusters"). We will illustrate the approach for the example of 3-clusters. In Hamiltonian (1) we also consider three-particle interactions U_3, but to simplify the equations we assume $U_4 = 0$, as above.

Expression (6) takes the form $\varepsilon' = \varepsilon_{1+2}' + \varepsilon_3'$, where

ε'_{1+2} is given by the right side of (13a), and ε'_3 is given by

$$\varepsilon_3' = \frac{1}{N_p}\sum_{i<j<k}\langle H_3^{ijk} - H_2^{ij} - H_2^{jk} - H_2^{ki} + 3H_1'\rangle. \qquad (17)$$

Here H_2^{ij} is $H_{2,r}$ from (13b) with $V_r = V_{ij}$, and the Hamiltonian (H_3^{ijk}) of the 3-cluster of pores i, j, k differs from (8a) with $\nu_k = 3$ only in the addition of a term with the ternary interaction $U_3^{ijk}\hat{n}_i\hat{n}_j\hat{n}_k$. The relationships among the fields $\psi_3^{(i)}$, $\psi_2^{(i)}$, and ψ_1 analogous to (13c) are

$$\psi_3^{(i)} = \psi_1 - \varphi_{ij} - \varphi_{ik} - \chi_{jk}^{\,i}, \quad \psi_2^{(i)} = \psi_1 - \varphi_{ij},$$
$$\psi_1 = \sum_j \varphi_{ij} + \sum_{j<k}\chi_{jk}^{\,i}, \qquad (18)$$

where the φ_{ij} are equal to φ_r from (13c) for $V_r = V_{ij}$, and $\chi_{jk}^{\,i}$ describes the nonbinary nature of the effect of pores j and k on pore i. The partition function of the 3-cluster, Z_3, is

$$Z_3^{ijk} = 1 + y_i + y_j + y_k + e_{ij}y_iy_j + e_{jk}y_jy_k + e_{ki}y_ky_i + e_{ijk}y_iy_jy_k, \qquad (19)$$

where

$$e_{ij} = \exp(-\beta V_{ij}), \quad e_{ijk} = \exp[-\beta(V_{ij} + V_{jk} + V_{ki} + U_3^{ijk})],$$

and the quantities $Y_i = Y_3^{(i)}$ are found from the nonlinear system of equations (9).

As a result we replace (15) by

$$\Omega = \Omega_1 + \frac{1}{2}\sum_{r=1}^{\infty} m_r\tilde{\Omega}_{2,r} + \frac{1}{N_p}\sum_{i<j<k}\tilde{\Omega}_3^{ijk}, \qquad (20a)$$

$$\mu = \mu_1 + \sum_{r=1}^{\infty} m_r\tilde{\mu}_{2,r} + \sum_{j<k}\tilde{\mu}_3^{ijk}. \qquad (20b)$$

Here the contributions of the ternary correlations are

$$\beta\tilde{\Omega}_3^{ijk} = -\ln Z_3^{ijk} - \beta(\tilde{\Omega}_2^{ij} + \tilde{\Omega}_2^{jk} + \tilde{\Omega}_2^{ki}) - 3\beta\Omega_1, \qquad (21a)$$

$$\beta\tilde{\mu}_3^{ijk} = \ln(y_iy_jy_k) - 2\beta(\tilde{\mu}_2^{ij} + \tilde{\mu}_2^{jk} + \tilde{\mu}_2^{ki}) - 3\beta\mu_1, \qquad (21b)$$

where $\tilde{\Omega}_2^{ij}$ and $\tilde{\mu}_2^{ij}$ mean $\tilde{\Omega}_{2,r}$ and $\tilde{\mu}_{2,r}$ from (16) with $V_r = V_{ij}$.

The higher-order correlations can be taken into account by examining ν-clusters with $\nu > 3$. This must be done in describing strong interactions with $\beta|V_{ij}| > 1$ (e.g., blocking), as we will see in Secs. 3 and 5. On the other hand, at $\beta|V_{ij}| \lesssim 1$ even the binary-cluster approximation turns out to be sufficiently accurate (Sec. 5).

3. BLOCKING MODEL WITH A WEAK [VAN DER WAALS] INTERACTION

To illustrate the influence of blocking effects on the thermodynamic properties of H in Me and to describe these effects in the cluster method, we consider a simplified model of a bcc hydride in this section. We assume that all the interactions beyond the blocking radius R_b are weak: V_{ij}, U_3, $U_4 \ll T$. If these conditions are assumed to hold up to the critical temperature T_c, then this model becomes an exact "lattice analog" of the van der Waals model of a nonideal gas[20] (this case was called the "high-temperature limit" in Ref. 6). The model also describes an α–α' phase transition of the gas-liquid type. By comparing the phase diagrams calculated in various versions of the cluster method with each other and with Monte Carlo calculations,[6] we can evaluate the accuracy of the methods.

As we mentioned above, the cluster method is equivalent to the mean-field approximation in the description of weak interactions with $|\beta V| \ll 1$. In accordance with this approximation, in all the terms in (1) which are nonlinear in $\hat{n}_i$, except the terms with the blocking interactions $V_{ij} = V_{ij}^b$, we write $\hat{n}_i$ as $c + \hat{x}_i$, where $\hat{x}_i = \hat{n}_i - c$, and we ignore the interaction of the fluctuations—terms of second and higher order in $\hat{x}_i$. Hamiltonian (1) becomes

$$H' = \sum_{i<j} V_{ij}^b\hat{n}_i\hat{n}_j + (w-\mu)\sum_i \hat{n}_i + \Omega_0(c), \qquad (22)$$

where

$$w = \gamma c + \gamma_3 c^2 + \gamma_4 c^3, \quad \Omega_0(c) = -{}^1/_2\gamma c^2 - {}^2/_3\gamma_3 c^3 - {}^3/_4\gamma_4 c^4, \qquad (23a)$$

$$\gamma = \sum_{j, R_{ij}>R_b} V_{ij}, \quad \gamma_3 = \sum_{j<k} U_3^{ijk}, \quad \gamma_4 = \sum_{j<k<l} U_4^{ijkl}. \qquad (23b)$$

In model (22) with $V_{ij} \gg T$, the thermodynamic potentials Ω and μ are evidently

$$\Omega = Tf_b(c) + \Omega_0, \quad \mu = Tg_b(c) + w. \qquad (24)$$

Here the functions $f_b(c)$ and $g_b(c)$ [which are related by (11): $f_b' = -cg_b'$] correspond to a model with only blocking interactions, which would naturally be called the "lattice hard-sphere model" by analogy with the models of nonideal gases.[6]

The functions $f_b(c)$ and $g_b(c)$ depend on only the blocking geometry in the lattice and can be calculated approximately by using clusters of various types. Corresponding calculations are described in the Appendix for crystals of the NbH_x type; their application in calculating the phase diagram for van der Waals model (22) (with $\gamma < 0$ and $\gamma_3 = \gamma_4 = 0$) is illustrated by Fig. 2 and Table I. Table I lists the critical concentrations and temperatures, x_c and T_c, for the gas-liquid phase transition, along with the concentrations corresponding to the densest random packing (of protons), x_{DRP}. For the ordinary hard-sphere model this con-

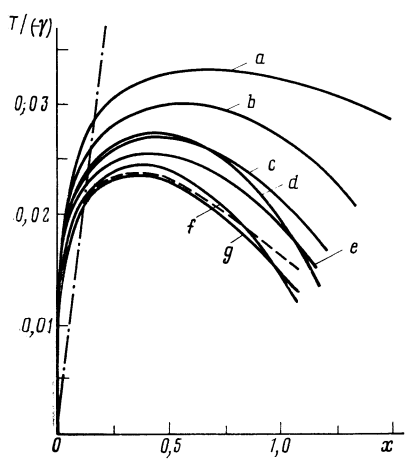

FIG. 2. $T_c(x)$ phase diagrams for van der Walls model (22) of hydrides of the NbH_x type in various approximations. Dot-dashed line—Mean-field approximation; curves a–g—cluster approximations a–g in Table IV; dashed line—Monte Carlo calculations.[6]

TABLE I. Values of the parameters x_c, T_c, and x_{DRP} for van der Waals model (22) of hydrides of the NbH_x type in various approximations

Approximation	Number of pores in the clusters	x_c	$-T_c/\gamma$	x_{DRP}
MFA	1	3	0,25	6
a	2, 1	0,682	0,0329	1,46
b	4, 2, 1	0,553	0,0301	1,34
c	4, 4, 2, 1	0,455	0,0269	1,21
d	5, 2, 1	0,452	0,0272	1,18
e	24, 2, 1	0,417	0,0254	1,16
f	8, 3	0,383	0,0245	1,08
g	24, 6, 2, 1	0,370	0,0236	1,075
Monte Carlo[6]	384	0,366	0,0237	1,09

cept was introduced by Bernal[21]; the corresponding value of the packing parameter (the ratio of the volume of a sphere to the average atomic volume) is $\eta_{DRP} = 0.64$ [by way of comparison, the equilibrium crystallization of a hard-sphere (HS) system occurs at[22] $\eta = 0.49$, while for the densest crystal packing we would have $\eta_{HS} = \pi\sqrt{2/6} = 0.74$]. In the lattice model under consideration here, (22), (24), we find the value of x_{DRP} from the vanishing of the entropy in (3): $s_H = -f_b/c - g_b = 0$. The quantity x_{DRP} evidently determines the maximum possible value of x at which H can still be in the disordered phase of a "lattice liquid" in the given structure: At $x > x_{DRP}$, only ordered structures of H are possible in Me. Correspondingly, the equilibrium curves $T_e(x) = T_{\alpha\alpha'}$ in Fig. 2 are drawn only up to $x = x_{DRP}$.

From Table I and Fig. 2 we see that (first) the simple mean-field approximation overestimates the values of x_c, T_c, and x_{DRP} in this system by an order of magnitude; i.e., this approximation is of no use for anything in the way of a quantitative estimate. Second, we see that the refinement of the description represented by increasing the clusters or choosing a more appropriate partitioning in the clusters leads to decreases in the calculated values of x_c, T_c, and x_{DRP}, apparently because of the more accurate description of the "excluded-volume" effects and the growth of the effective size of each proton in the lattice. Third, we see that the partitioning into clusters of type *g* which is described in the Appendix is generally the most natural of the partition procedures considered, since each of the Me atoms is the center of a regular 24-cluster, while the clusters of smaller size are added (or subtracted) only to satisfy (6). We see from Table I and Fig. 2 that for this partitioning the results on x_c, T_c, and $T_e(x)$ [and also on the functions $f_b(c)$ and $g_b(c)$] at $x \lesssim 0.7$ are essentially the same as those found by the Monte Carlo calculations.[6] At larger values of x the functions $f_b(c)$, $g_b(c)$, and $T_c(x)$ begin to diverge slightly from those calculated by an interpolation of the Monte Carlo calculations of Ref. 6, apparently because this interpolation becomes less accurate at large values of x, as mentioned in Ref. 6.

Nevertheless, on the whole Table I and Fig. 2 show that even for the extremely simple clusters of types *c*, *d*, and, especially, *f*, the accuracy of the results is quite high. Accordingly, in the discussion below of some models for hydrides which are more realistic than the van der Waals model we will for simplicity describe the influence of the blocking interactions by means of 5-clusters of type *d*.

4. ESTIMATES FOR THE H–H INTERACTIONS IN Nb AND Pd

As we mentioned in the Introduction, the V_{HH} interactions in Me are assumed by convention to consist of stress-induced and screened Coulomb components V_{si} and V_e. We will discuss these components for the particular cases of the NbH_x and PdH_x systems, which have received the most study. We wish to determine the nature and the relative roles of the V_{si} and V_e components in bcc and fcc hydrides. We will use the results to calculate thermodynamic properties in Sec. 5.

In finding V_{si} we will for simplicity consider only the incoherent states of the crystal,[6,9] and we will use the ordinary equations of the harmonic approximation [see, e.g., (2.9) in Ref. 6 or (38.20) in Ref. 23], assuming a linearity and a superposition of the displacements of the Me atoms induced by the various protons. In the calculations for Nb, we use the same lattice constants and the same dipole-elastic tensor as in Ref. 6, while for the phonon spectra $\omega(\mathbf{k})$ we use the data of Ref. 24. The values found for $V_{si}(\mathbf{R})$ are shown in Table II. In this table, $\mathbf{R}$ is measured from pore 7 in Fig. 1; m_r is the coordination number in the *r*th coordination sphere; and $\gamma = \gamma_{4\text{-}\infty}$ is the constant of the mean-field approximation from (23b) (with a summation over $R_{ij} > R_b$, i.e., over $r \geqslant 4$), which characterizes the "average" interaction. The values of V_{si} in Table II differ from those found in Refs. 6 and 10 [where older data[25] on $\omega(\mathbf{k})$ were used] by 10–15% but exhibit the same qualitative behavior.

It can be seen from this table that the values of $V_{si}(\mathbf{R})$ vary rapidly as the magnitude and direction of $\mathbf{R}$ change; as we go from $r = 10a$ to $r = 10b$, for example, the weak attraction gives way to a strong repulsion. This behavior is determined primarily by geometric factors. In this model, in which the H–Me interaction is taken into account in only two coordination spheres, the proton is primarily a dilatation center, and it repels the neighboring Me atoms. Accordingly, if two protons are present on different sides of the same Me atom, the interaction V_{si} between these protons will be strongly repulsive, as at $r = 10b$ (between pores 7 and 14 in Fig. 1). If, on the other hand, the Me atoms lie beside the bond (as for $r = 1$, 2, 3 or $r = 10a$, for example; i.e., for

TABLE II. Estimates for H–H interactions in Nb

r	$\frac{4R}{a}$	m_r	V_{si}, K	V_e, K				
				$\varepsilon(q)$				
				GT [27], $z_e=4$	GT [27], $z_e=3$	GT [27], $z_e=2$	VS [28], $z_e=4$	Nonlinear ε (Ref. 18), $z_e=3.5$
1	101	4	−3249	3559	3170	3095	3469	3100
2	002	2	−2160	1374	904	−344	756	210
3	211	8	−1330	627	838	572	287	330
4	220	4	−618	−128	309	665	−93	330
5	301	8	−429	−196	−93	336	−188	130
6	222	8	−227	−120	−220	−161	−106	−30
7	123	16	126	14	−163	−192	5	–
8*a*	004	2	−197	94	−44	−235	68	–
8*b*	400	4	449	94	−44	−235	68	–
9*a*	033	4	577	100	55	−182	73	–
9*b*	141	8	626	100	55	−182	73	–
10*a*	402	4	−59	58	102	−89	41	–
10*b*	042	4	822	58	102	−89	41	–
11	323	8	15	4	100	3	0	–
12	224	8	−30	−37	66	70	−30	–
$\gamma=\sum_{r=4}^{\infty} m_r V_r$			−8300	−1028	−2050	−4686	–	–

the bond between pores 7 and 9′ in Fig. 1), then the tendency of the lattice of Me atoms to maintain a constant average density gives rise to compressional forces along the bond, i.e., an effective H–H attraction. In the harmonic approximation used here, the displacements of the Me atoms induced by each proton add up in a linear manner; i.e., the anharmonicity effects which limit these displacements are ignored. As a result, for small R (in particular, for $r=1, 2, 3$), the calculated attractive forces turn out to be very large.

We turn now to the $V_e(\mathbf{R})$ interaction. In their study of phase transitions in NbH_x, Horner and Wagner[6] and Futran *et al.*[10] assumed that V_e gives rise to the observed blocking at $r=1, 2$, and 3 and is small at $r\geqslant 4$, but they did not calculate V_e. We have carried out such calculations, in the approximation of a linear screening [see, for example, Eq. (1) in Ref. 26], which ignores the inhomogeneity of the electron density in the metal and also terms of higher order in the *e*–H interaction. Nevertheless, this approximation can be used for a qualitative discussion. We used various approximations for the dielectric function $\varepsilon(q)$ (Refs. 26–29), and we varied the number of screening electrons (z_e) at the Me atom. The last column in Table II also shows the results calculated for V_e with a nonlinear screening (taking from Fig. 1 in Ref. 18), i.e., without the use of a perturbation theory in the *e*–H interaction. For a homogeneous electron gas, these results should be regarded as more accurate than those found in the approximation of linear screening, but in a metal the presence of the strong *e*–Me bond should reduce the polarizability of the electrons caused by an impurity proton, and models with linear $\varepsilon(q)$ may also have realistic features.

From the results of these calculations of V_e, illustrated in Table II, we can draw several conclusions.

1. When the harmonic approximation, (26), is used for V_{si}, it is not possible to describe the observed blocking effect with any realistic V_e; i.e., it is not possible to derive values $(V_{si}+V_e)_r \geqslant T_c \approx 450$ K with $r=1, 2, 3$ in Table II. A nonlinear screening[18] for all $z_e \gtrsim 1$ leads to a repulsion even weaker than that found with linear screening. The band calculations of Ref. 19 also indicate that the screening of H in Me is important. It can thus be assumed that the blocking is due to a pronounced anharmonicity of the stress-induced interactions at small values of R and the inapplicability of the general expressions for V_{si} from Refs. 6 and 23 in this case. Qualitative confirmation of this assumption comes from the circumstance that the displacements of the Me atoms with respect to the H in NbH_x are not small, even around a single proton: $\delta R_{MeH} \approx 0.1$ Å (Ref. 30). For two neighboring protons, the superposition of such displacements would give us $\delta R_{MeH}/R_{MeH} \gtrsim 0.1$, which probably exceeds the applicability limit of the harmonic approximation in Nb. Consequently, in the statistical calculations in Sec. 5 we use $V(\mathbf{R})$ from Table II only for $r\geqslant 4$; for $r=1, 2, 3$, we assume there is a blocking.

2. For realistic interactions V_e (e.g., for the GT approximation[27] or the VS approximation[28] of ε with $z_e = 3$–4 or for the nonlinear ε in Table II) we usually have $|V_{si}| > |V_e|$. For quantitative calculations, however, V_e must be taken into account.

3. The interactions $V_{HH}(\mathbf{R}) = V_{si} + V_e$ are oscillatory and not small in comparison with T_c up to $r = 10b$, and they fall off rather slowly with increasing R at large R.

In Table III we show the results calculated for $V_{HH}(\mathbf{R})$ for Pd. We took the values of V_{si} for this metal from the calculations of Ref. 9, while the linear screening V_e was found in the same way as above, by varying z_e from 1 to 9. The nonlinearly screened interactions $(V_e)_{nls}$ are given in Ref. 18 only for $R \lesssim R_1 = 2.8$ Å; here $(V_e)_{nls} \lesssim 20$ K.

It can be seen from Table III that the maximum values of $|V_{si}|$ in the fcc hydrides are much smaller than in the bcc hydrides (because the pore density per Me atom is lower by a factor of six), and at all values of R we have $|V_{HH}(R)| \lesssim T_c \approx 565$ K. In this connection, the simple mean-field approximation turns out to be generally applicable for evaluating statistical properties here, although in quantitative calculations the substantial and oscillating potentials V_r in the first three spheres require more accurate methods,

TABLE III. Estimates for H–H interactions in Pd

r	$\frac{2R}{a}$	m_r	V_{si}, K	V_e, K, $\varepsilon(q)$: GT, $z_e=2$	GT, $z_e=3$	GT, $z_e=4$	VS, $z_e=2$
1	110	12	−186	−73	−202	−66	−132
2	200	6	305	95	34	−51	70
3	211	24	−120	−39	−15	33	−30
4	220	12	79	−6	20	−21	−3
5	310	24	21	29	−21	11	21
6	222	8	28	−16	9	0	−12
7	321	48	−11	−12	7	−8	−9
8	400	6	−27	13	−10	7	10
9*a*	330	12	10	8	−1	2	6
9*b*	411	24	5	8	−1	2	6
10	420	24	−1	−8	7	−6	−6
$\gamma_{1-10}=\sum_{r=1}^{10} m_r V_r$			−2078	−1139	−2383	−733	−1775

e.g., cluster methods. It can also be seen that although $|V_{si}|$ is usually greater than $|V_e|$, as in Nb, the "average" interactions γ_{si} and γ_e are comparable. The thermodynamic properties here are thus much more sensitive to the form of V_e than in bcc hydrides.

5. CALCULATIONS OF GAS–LIQUID PHASE DIAGRAMS IN NbH_x AND PdH_x

In this section we use the methods of Sec. 2 and 3 to describe incoherent[6,2] gas–liquid phase transitions in NbH_x and PdH_x, using the estimates of the interactions V_{HH} from Sec. 4. We will show that even for models of the hydrides more realistic than the van der Waals model (Sec. 3) the cluster approximation yields accurate calculations of the statistical properties. A comparison of the calculated results with experimental data also leads to certain qualitative conclusions about the interactions of H in Me, in particular, the conclusion that there are significant nonbinary or concentration-dependent forces among protons.

As we noted earlier, in PdH_x the interactions V_{HH} in Table III are not comparable to T_c, and the very simple approximations of 2- and 3-clusters [(15) and (20)] seem to be sufficient for describing this system. In NbH_x, however, many of the interactions $V_{HH}(R)$ exceed T_c, and, in accordance with the discussion in Secs. 2 and 3, the expressions for Ω and μ in this case are written as the sums of contributions from short-range (in particular, blocking) interactions Ω_s, μ_s and from the interactions of more remote neighbors, Ω_l, μ_l:

$$\Omega=\Omega_s+\Omega_l, \quad \mu=\mu_s+\mu_l. \tag{25}$$

For Ω_s we use the approximation of 5-clusters (see Sec. d in the Appendix) containing only blocking interactions. From Table IV in the Appendix we have

$$\beta\Omega_s^{(5)}=\ln(1-c)+2\ln\frac{1-2c}{(1-c)^2}+\frac{1}{2}\ln\frac{1-5c}{(1-c)^5}$$
$$\beta\mu_s^{(5)}=\ln\frac{c}{1-c}+4\ln\frac{1-c}{1-2c}+\frac{5}{2}\ln\frac{1-c}{1-5c}. \tag{26}$$

The Ω_s contribution can be taken into account more accurately by using the 8-clusters described in Sec. f of the Appendix (Fig. 2 and Table I). This refinement is easy to make in more detailed, quantitative calculations. Here, on the other hand, we will be discussing qualitative questions for the most part, and we will use simple expressions (26) for Ω_s and μ_s.

The contributions of nonblocking interactions Ω_l are described in three approximations: *A*) the approximation of binary clusters [with a summation over $r\geqslant 4$ in (15)]; *B*) the approximation of 2- and 3-clusters [with a summation in (20) over clusters of pores i, j, k with $R_{ij}, R_{jk}, R_{ki} > R_b$]; and *C*) the approximation in which the contributions of V_r with $r = 4$, 6, 8*b*, and 10*b* are described by means of 8-clusters of pores 1, 3, 7, 9, 11, 12, 13, 14 and 4-clusters of pores 1, 3, 7, and 9 in Fig. 1 (called "8*c*-clusters" and "4*c*-clusters" below), while binary clusters (16) are used for the other values $r\geqslant 5$.

Approximation *C* was chosen because these interactions V_r are large according to the estimates in Table II; for example, $V_{10b}|V_4|\gtrsim 2T_c$. It is thus interesting to compare the results found in a description of these contributions to the thermodynamics in the approximation of binary clusters, (16), and of 8*c*-clusters and 4*c*-clusters, which apparently take into account the most important of the nonbinary correlations. The expressions for Ω_l and μ_l in approximation *C* are

$$\beta\Omega_l=\frac{1}{2}{\sum_{r\geqslant 5}}' m_r\beta\tilde{\Omega}_{2,r}+2\beta\tilde{\Omega}_{2,6}-\frac{1}{2}\ln Z_{8c}+\ln Z_{4c},$$
$$\beta\mu_l={\sum_{r\geqslant 5}}' m_r\beta\tilde{\mu}_{2,r}+4\beta\tilde{\mu}_{2,6}+4(\ln y_{8c}-\ln y_{4c}). \tag{27}$$

Here the prime means that the sum does not contain terms with $r = 6$, 8*b*, and 10*b*. The expressions for $\tilde{\Omega}_2$ and $\tilde{\mu}_{2,r}$ are the same as in (16). The partition functions for the clusters, $Z_{8c}(y_{8c}, T)$ and $Z_{4c}(y_{4c}, T)$, are given by

$$Z_{8c}(y,T)=1+8y+4y^2(2e_4+2e_6+e_8+e_{10})+8y^3(e_4^2e_8+2e_4e_6e_{10}+e_6^2e_8)+2y^4(e_4^4e_8^2+4e_4^2e_6^2e_8e_{10}+2e_4^2e_6^2e_{10}^2+e_8^2e_{10}^4),$$
$$Z_{4c}(y,T)=1+4y+2y^2(e_4+e_6), \tag{28}$$

where

$$e_4=\exp(-\beta V_4),\quad e_6=\exp(-\beta V_6),\quad e_8=\exp(-\beta V_{8b}),$$
$$e_{10}=\exp(-\beta V_{10b}),$$

and $y_{8c}=y(c,T)$ and $y_{4c}=\tilde{y}(c,t)$ are found from Eqs. (9):

$$c=\tfrac{1}{8}y\frac{\partial}{\partial y}\ln Z_{8c}(y,T),\qquad c=\frac{1}{4}\tilde{y}\frac{\partial}{\partial\tilde{y}}\ln Z_{4c}(\tilde{y},T). \quad (29)$$

Phase-equilibrium curves $T=T_c(x)$ are found from Eqs. (4). The sums over r in (15) and (27) are calculated from (16) up to a final $r=r_m$, and the remainder, Ω_m or μ_m, is replaced by the expression from the mean-field approximation in accordance with the comment following Eqs. (16):

$$\Omega_m=-\frac{1}{2}\gamma_m c^2,\qquad \mu_m=\gamma_m c,\qquad \gamma_m=\sum_{r=r_m+1}^{\infty} m_r V_r. \quad (30)$$

In the calculations for NbH_x we set $r_m=16$, and in those for PdH_x we set $r_m=10$. In the calculations of the 3-cluster contribution, (21), on the other hand, the sums over i, j, and k in (20) extend up to $r_m^{(3)}=4R_m/a\sqrt{2}=12$ in NbH_x, while those in PdH_x extend up to $r_m^{(3)}=2R_m a/\sqrt{2}=2$, where $R_m=\max(R_{ij},R_{jk},R_{ki})$, and a is the lattice constant; the remainder is discarded.

Figure 3 compares the results calculated on $T_c(x)$ for NbH_x in the various approximations for Ω_l [we use expressions (26) for Ω_s, while for the constants $V_{HH}(R)$ we use the values $V_{si}(R)$ from Ref. 6] with the results of Monte Carlo calculations,[6] which used a finite grid of $N_p=384$ pores and periodic boundary conditions (the presence of large long-range forces can slow the convergence of the results of the simulation at a finite N_p to the statistical limit $N_p\to\infty$; these questions were not discussed in Ref. 6). Comparison of curves A, B, and C shows that the approximation of binary clusters gives a sufficiently accurate description of the Ω_l contributions, and the incorporation of multiparticle correlations results in comparatively small corrections. We also see that the results of all the cluster approximations agree quite well with the Monte Carlo results.[6] In contrast, the description of Ω_l in the mean-field approximation, i.e., the description by means of Eqs. (22)–(24) with $\gamma_3=\gamma_4=0$ (curve D), underestimate $T_c(x)$ greatly in comparison with the cluster approximations. The reason is that for the values of βV_r under consideration here which are not small, the replacement (Sec. 2) of expressions of the type $\exp(-\beta V_r)$ by their expansion $1-\beta V_r$ in the mean-field approximation results in a large error.

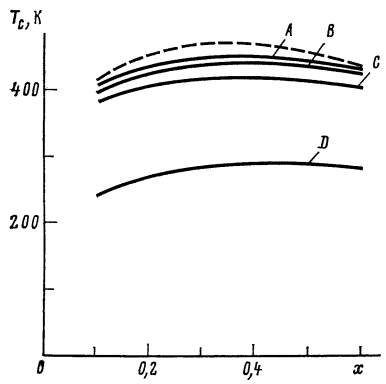

FIG. 3. $T_c(x)$ phase diagrams calculated for NbH_x with $V_{HH}(\mathbf{R})=V_{si}(\mathbf{R})$ from Ref. 6. Dashed line—Monte Carlo calculations: Lines A, B, C, and D correspond to the use of expression[26] for Ω_s, while approximations A, B, C (see the text proper), and the mean-field approximation are used for Ω_l.

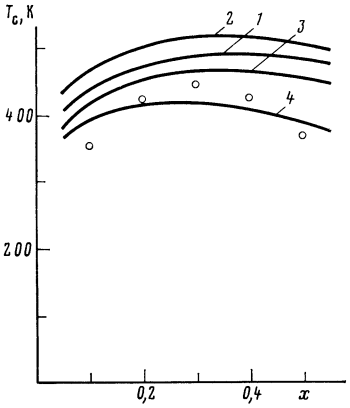

FIG. 4. $T_c(x)$ phase diagrams calculated for NbH_x with $V_{HH}=V_{si}+V_e$ from Table II, with the GT approximation of $\varepsilon(q)$, and with[26] for Ω_s. The curves correspond to the following values of z_e and the following approximations for Ω_l: 1—$z_e=3$, A; 2—$z_e=4$, A; 3—$z_e=4$, C; 4—$z_e=4$, C to which a 3- and 4-particle repulsion is added (see the text proper). The points are experimental.[7]

In the calculations shown in Fig. 4 we used the more realistic interactions $V_{HH}=V_{si}+V_e$ with V_{si} and V_e from Table II. For V_e we used the linear-screening approximation (27) with the GT approximation of $\varepsilon(q)$. Comparison of curves 1 and 2 shows that a variation of the density of screening electrons (the switch from $z_e=3$ to $z_e=4$) for NbH_x does not have a great effect on the results, because of the relatively large values of V_{si}. We also see that the "average interaction" γ in the last row of Table II falls far short of giving a complete characterization of the interaction (as in the mean-field approximation). For $z_e=3$, for example, the average attraction $(-\gamma)$ is larger, but the values of $T_c(x)$ are smaller, than for $z_e=4$. Incorporating the many-particle correlations in the approximation of $8c$- and $4c$-clusters changes the results to a greater extent than in Fig. 3, but on the whole the changes are still not great.

Above we discussed some methodological questions involving the accuracy of the calculations with the particular interaction models chosen. If we now compare the calculations with experiment (Fig. 4) we see that at values $x\lesssim x_c$ (not very large) these models give a fairly good description of the observed behavior $T_c(x)$. At larger values of x, however, the theoretical values of T_c in Figs. 3 and 4 fall off more slowly with x than do the experimental values. This discrepancy was also noted by Horner and Wagner,[6] who suggested that it might be due to the $V_e(R)$ interactions which they ignored. We have carried out detailed calculations of $T_c(x)$ for NbH_x, varying V_e over a very broad range, using both the approximation of linear screening for a wide variety of $\varepsilon(q)$ and z_e and also other physically plausible forms of $V_e(R)$. In all cases, the calculated values of T_c fell off more slowly than the experimental values at large values of x; this situation

seems to be characteristic of all models with purely binary interactions $V_{HH}(R)$.

We accordingly studied the effect on $T_e(x)$ of various possible nonbinary interactions of the U_3 and U_4 type in Hamiltonian (1). Such terms arise, for example, when we take into account the anharmonicity of the displacements δR_{MeH} (Ref. 31); the results of a numerical simulation[16] show that this "anharmonic" deviation from binary interactions may be significant. In accordance with the comments in Sec. 4, there is the possibility that in systems of the NbH_x type these effects will correspond primarily to a repulsion (in comparison with the results of the harmonic approximation). To obtain some estimates we modeled this repulsion by setting $U_3^{ijk} = U_3$, $U_4^{ijkl} = U_4$ for $R_m < R_c$ in (1) and $U_3 = U_4 = 0$ at $R_m > R_c$, where R_m in the maximum distance between pores i, j, k, l; and U_3, U_4, and R_c are constants.

We found that even extremely small values of U_3 and U_4 noticeably improved the agreement of $T_e(x)$ with experiment. The improvement is illustrated by curve 4 in Fig. 4, obtained with $U_3 = U_4 = 30$ K and $R_m = 3a\sqrt{2}$. Since U_3 and U_4 are small, we can calculate these contributions to Ω and μ in the mean-field approximation, i.e., from expressions like (22) and (23), as we did in the calculations.

Consequently, at $x \lesssim x_c$ the phase diagrams for systems of the NbH_x type can apparently be described satisfactorily by the models of Sec. 4, while at larger values of x the deviation from purely binary interactions becomes significant.

Figure 5 shows $T_e(x)$ diagrams for PdH_x. A comparison of curves 1 and 2 again reveals a fairly good agreement between the results of Monte Carlo calculations[9] and the results of the 2-cluster approximation. The approximate agreement of curves 3 and 4 confirms that for the substantial values $\beta|V_r| \lesssim 1$ considered here the 2-cluster approximation is apparently sufficiently accurate, and many-particle correlations are of minor importance. As was mentioned above (and also in a previous study[9]), however, the values of $V_{HH}(R)$ and the thermodynamic results are less sensitive to the form of V_e here than in the bcc hydrides; the situation is illustrated by curves 3 and 5 in Fig. 5. At large values of x, the calculated values of $T_e(x)$ fall off more slowly with x than do the experimental results, as in the case of NbH_x. This result is further evidence that there are important nonbinary forces and/or contributions of other, e.g., band, effects, as has been discussed by many investigators for the case of PdH_x [see, e.g., Refs. 8, 16, and 2 (Vol. 2, Chapter 2)].

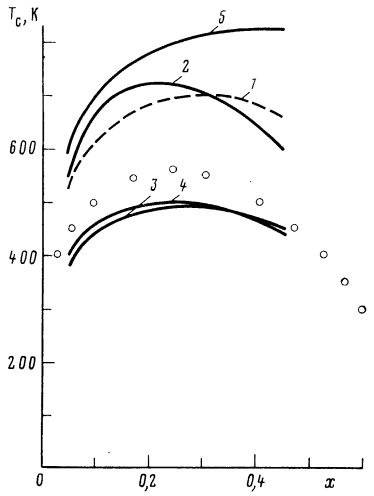

FIG. 5. $T_e(x)$ phase diagrams calculated for PdH_x for the following interactions $V_{HH}(\mathbf{R})$ and the following approximations for Ω: 1—V_{HH} from Ref. 9, Monte Carlo calculations; 2—the same V_{HH}, 2-clusters; 3—$V_{HH} = V_{si} + V_e$ from Table III with $\varepsilon(q)$ in the GT approximation with $z_e = 2$, 2-clusters; 4—the same V_{HH}, 2- and 3-clusters, (20); 5—the same as for curve 3, but with $z_e = 3$. The points are experimental.[8]

Consequently, again in the case of hydrides of the PdH_x type the cluster approximation can apparently yield accurate results on the configurational contributions to the thermodynamics, and a comparison of these calculations with experiment can be used to refine the estimates regarding H–H interactions.

6. CONCLUSION

We have discussed primarily methodological and qualitative aspects of the theory for H in Me. We have shown that the form of the cluster approximation which has been proposed combines simplicity with high practical accuracy and is convenient for calculations of statistical properties. The methods which have been developed are evidently applicable not only to H in Me but also to any other thermodynamically equilibrium interstitial systems. We have also estimated the stress-induced and electron contributions to the H–H interactions, and we have carried out calculations with these interactions V_{HH} for the gas-liquid phase transitions in NbH_x and PdH_x. These estimates and calculations indicate that anharmonic Me–H interactions are important (especially in the bcc hydrides), apparently giving rise to both blocking effects at small values of R and significant nonbinary interactions of the protons.

More-detailed information on the H–H interactions can be acquired by applying these methods to other problems of the physics of H in Me. We might single out as the most important of these problems a description of the thermodynamic characteristics of H in Me: $\mu(x, T)$, the entropy $s_H(x, T)$, and the enthalpy $h_H(x, T)$, on which we have extensive experimental information.[2,8,16] These methods can also be used to describe ordered phases of H in Me and the phase transitions to these phases, e.g., the α-β (or α'-β) phase transition to the MeH structure in NbH_x (Refs. 1 and 2). Equations (6) and (12) in this case are generalized to incorporate the existence of several nonequivalent H sublattices in the ordered phase. Preliminary results for the $T_{\alpha\beta}(x)$ and $T_{\alpha'\beta}(x)$ equilibrium curves [as for $\mu(x, T)$ in the thermodynamic calculations] again point to the importance of may-particle or concentration-dependent interactions in NbH_x. For purely binary interactions, for example, the concentration interval in which the MeH phase exists turns out to be very narrow: $|1 - x| \lesssim 0.03$. However, the use of the small admixture of 3- and 4-particle interactions as mentioned above leads to a natural description of the wide range of existence which has been observed experimentally[7] for this phase: $|1 - x| \approx 0.3$.

The methods described above can also be used to study the short-range order and correlations of H in Me, which

have so far been discussed only in the mean-field approximation.[23] The cluster method makes it possible to study these questions at a more quantitative level and to obtain information about the H–H interactions from data on diffuse scattering by hydrides. All these questions will be discussed in other papers.

We would also like to comment on the possible use of the results of Sec. 3 to predict certain features of the phase diagrams of hydrides of the NbH_x type. As was mentioned above, at $x > x_{DRP}$ these systems may not remain disordered as the tetrapores are filled and as blocking occurs; the same is evidently true when the nonblocking interactions are taken into account more accurately than in the mean-field approximation. Accordingly, the range over which "liquid-like" phase α' exists in these systems must be bounded by the condition $x < x_{DRP} \approx 1.07$. The experimental NbH_x phase diagram agrees with this prediction, revealing in particular a sharp—nearly vertical—increase in the boundary of the α' phase at $x \approx 0.9$. However, for TaH_x, for example, this part of the phase diagram has not yet been studied.[7] In accordance with the discussion above, here again we should observe a sharp increase in the right-hand boundary of the α' phase, and an experimental test of this prediction, i.e., of the applicability of this blocking model to the case of TaH_x also, appears to be extremely interesting.

We deeply thank V. A. Somenkov, S. Sh. Shil'shteĭn, and A. V. Irodova for many discussions which have stimulated this study.

APPENDIX

Calculation of Ω and μ in the cluster approximations for the "lattice hard-sphere model" in crystals of the NbH_x type

In this model, blocking occurs in the first three coordination spheres, with coordination numbers $m_1 = 4$, $m_2 = 2$, and $m_3 = 8$ (Fig. 1), and the exact expression for ε' in (6) is

$$\varepsilon' = \langle 2V_1^b \hat{n}_1\hat{n}_2 + V_2^b \hat{n}_1\hat{n}_3 + 4V_3^b \hat{n}_1\hat{n}_5 - \mu\hat{n}_1\rangle. \quad \text{(A1)}$$

Here the pores are numbered in accordance with Fig. 1, and we are assuming $V_i^b \gg T$. We wish to describe the calculations of Ω and μ [i.e., of the functions f_b and g_b in (24)] using clusters of various types. As in Sec. 2, we call a cluster of ν pores a "ν-cluster," and we set the index k in Eqs. (6)–(12) equal to ν. The results are listed in Table IV.

a) 2-clusters. The quantities Ω and μ are given by (15) and (16), in which we have $f_r = -1$ for $r \leqslant 3$ and $f_r = \tilde{\Omega}_{2,r} = \tilde{\mu}_{2,r} = 0$ for $r \geqslant 4$.

b) A 4-cluster of pores 1, 2, 3, 4 and a 2-cluster of pores 1, 6 (Fig. 1). The fields ψ_k in the clusters are related by $\psi_1 = 4\varphi_1 + 2\varphi_2 + 8\varphi_3$, $\psi_2 = \psi_1 - \varphi_3$, $\psi_4 = \psi_1 - 2\varphi_1 - \varphi_2$. The results for Ω and μ are found by substituting the solutions of (9) into (10) and (12): $y_2 = c(1-2c)^{-1}$, $y_4 = c(1-4c)^{-1}$.

c) 4-clusters of pores 1, 2, 3, 4 ($k = 4a$) and 3, 4, 5, 5′ ($k = 4b$) and an 2-cluster of pores 1, 6 (Fig. 1). The calculations (as for Subsection d below, are analogous to those in Subsection b.

d) A 5–cluster of pores 1, 2, 4, 5, 5′ and a 2-cluster of pores 1, 6 (Fig. 1).

e) A 24-cluster consisting of pores lying on all six faces of the unit cube of the bcc lattice of the Me atoms in Fig. 1 (the 2-cluster corresponds to pores 1, 2). The blocking conditions allow no more than five protons in the 24-cluster, and Z_{24} is given by

$$Z_{24} = 1 + 24y + 180y^2 + 472y^3 + 366y^4 + 48y^5, \quad \text{(A2)}$$

where $y = y_{24}(c)$ is determined by Eq. (9):

$$c = \frac{1}{24} y \frac{d}{dy} \ln Z_{24}(y). \quad \text{(A3)}$$

f) An 8-cluster of pores 1, 2, 3, 4, 5, 5′, 8, 8′ and a 3-cluster of pores 1, 2, 3 (Fig. 1). The 8-cluster contains pores of three nonequivalent types with the fields $\psi_8^{(1)} = \psi_8^{(4)}$, $\psi_8^{(2)} = \psi_8^{(3)}$, and $\psi_8^{(5)} = v_8^{(5')} = \psi_8^{(8)} = \psi_8^{(8')}$, while the 3-cluster contains two types, with the fields $\psi_3^{(1)} = \psi_3^{(3)}$ and $\psi_3^{(2)}$. Since there are five nonequivalent pores, the number of variational parameters of the problem can be increased, and we do not have to assume a simple additivity of the fields φ_1, φ_2, φ_3 acting on a pore along each of the bonds [formally, this increase is required, since for the five equations (9) to be solvable with a given c we need at least four variables φ in addition to μ]. Along with the "one-particle" fields $\varphi_1, \varphi_2, \varphi_3$, we introduce the field φ_t, which is the field exerted on a given pore, (1), by the triad of bonds (1–2, 1–3, and 1–4), under the general assumption $\varphi_t \neq 2\varphi_1 + \varphi_2$. We then have

$$\begin{aligned} &\psi_3^{(1)} = \varphi_t + \varphi_1 + 8\varphi_3, \quad \psi_3^{(2)} = \varphi_t + \varphi_2 + 8\varphi_3, \\ &\psi_8^{(1)} = \varphi_2 + 6\varphi_3, \quad \psi_8^{(2)} = \varphi_t + 6\varphi_3, \quad \psi_8^{(5)} = \varphi_t + \varphi_1 + 6\varphi_3. \end{aligned} \quad \text{(A4)}$$

TABLE IV.

Approximation	Number of pores in the clusters	Values of Λ_k in (10)	$\beta(\Omega_b - \Omega_1) = f_b(c) - \ln(1-c)$	$\beta(\mu_b - \mu_1) = g_b(c) - \ln[c/(1-c)]$
a	2, 1	–	$7f_2$	$7g_2$
b	4, 2, 1	$\lambda_4 = 1/2$, $\lambda_2 = 4$, $\lambda_1 = -9$	$4f_2 + 1/2 f_4$	$4g_2 + 1/2 g_4$
c	4, 4, 2, 1	$\lambda_{4a} = 1/2$, $\lambda_{4b} = 4$, $\lambda_2 = -2$, $\lambda_1 = -1$	$-2f_2 + 3/2 f_4$	$-2g_2 + 3/2 g_4$
d	5, 2, 1	$\lambda_5 = 1/2$, $\lambda_2 = 2$, $\lambda_1 = -11/2$	$2f_2 + 1/2 f_5$	$2g_2 + 1/2 g_5$
e	24, 2, 1	$\lambda_{24} = 1/12$, $\lambda_2 = -1$, $\lambda_1 = 1$	$-f_2 + 1/12 L_{24}$	$-2\ln y_2 + 2\ln y_{24}$
f	8, 3	$\lambda_8 = 1/2$, $\lambda_3 = -1$	$-2f_3 + 1/2 f_4 + f_5$	$-2g_3 + 1/2 g_4 + g_5$
g	24, 6, 2, 1	$\lambda_{24} = 1/6$, $\lambda_6 = -2/3$, $\lambda_2 = -1$, $\lambda_1 = 3$	$-f_2 - 2/3 L_6 + 1/6 L_{24}$	$-g_2 - 4\ln y_6 + 4\ln y_{24}$

Solving Eqs. (9), we find

$$y_3^{(1)}=y_3^{(2)}=\frac{c}{1-3c}, \quad y_8^{(5)}=\frac{c}{1-5c},$$
$$y_8^{(2)}=\frac{c(1-3c)}{(1-4c)(1-5c)}, \tag{A5}$$
$$y_8^{(1)}=\frac{c(1-3c)^2}{(1-4c)(1-5c)^2}, \quad Z_8=\frac{(1-3c)^2}{(1-4c)(1-5c)^2}.$$

Now using (10) and (12), we find the results in row *f* in Table IV.

g) A 24-cluster which is the same as in Subsec. e; a 6-cluster of pores 1, 2, 5, 6, 7, 8; and a 2-cluster of pores 1, 3. The values of Z_{24} and y_{24} are given by (A2) and (A3), while Z_6 and y_6 are given by

$$Z_6=1+6y_6+3y_6^2, \quad y_6=[(1-8c+24c^2)^{1/2}-1+6c]/2(1-3c). \tag{A6}$$

The resulting expressions for Ω and μ are listed in Table IV, where we have used the following notation:

$$f_k=\ln\frac{1-kc}{(1-c)^k}, \quad g_k=k\ln\frac{1-c}{1-kc}, \quad L_k=-\ln Z_k-k\ln(1-c). \tag{A7}$$

[1]V. A. Somenkov and S. Sh. Shil'shteĭn, Fazovye prevrashcheniya vodoroda v metallakh (Phase Transitions of Hydrogen in Metals). Preprint I. V. Kurchatov Institute of Atomic Energy, Moscow, 1978; Prog. Mater. Sci. **24**, 267 (1980).
[2]G. Alefeld and J. Völkl (editors), Hydrogen in Metals (Russ. transl. Mir. Moscow, Vols. 1 and 2, 1980).
[3]E. G. Maksimov and O. A. Pankratov, Usp. Fiz. Nauk **116**, 385 (1975) [Sov. Phys. Usp. **18**, 481 (1975)].
[4]T. D. Lee and C. N. Yang, Phys. Rev. **87**, 410 (1952).
[5]K. Huang, Statistical Mechanics, Wiley Press, New York (1965) (Russ. transl. Mir. Moscow, 1966).
[6]H. Horner and H. Wagner, J. Phys. C **7**, 3305 (1974).
[7]U. Köbler and J.-M. Welter, J. Less Common Met. **84**, 225 (1982).
[8]T. Kuji, W. A. Oates, B. S. Bowerman, and T. B. Flanagan, J. Phys. F **13**, 1785 (1983).
[9]S. Dietrich and H. Wagner, Z. Phys. **36**, 121 (1979).
[10]M. Futran, S. G. Coates, C. K. Hall, and D. O. Welch, J. Chem. Phys. **77**, 6223 (1982).
[11]D. J. Picton, R. A. Bond, B. S. Bowerman, *et al.*, J. Less Common Met. **88**, 133 (1982).
[12]A. G. Khachaturyan and G. A. Shatalov, Acta Metall. **23**, 1089 (1975).
[13]V. G. Vaks, Vvedenie v mikroskopicheskuyu teoriyu segnetoélektrikov (Introduction to the Microscopic Theory of Ferroelectrics), Nauka, Moscow, §17, 1973, p. 24.
[14]V. G. Vaks and N. E. Zeĭn, Zh. Eksp. Teor. Fiz. **67**, 1082 (1974) [Sov. Phys. JETP **40**, 537 (1975); Fiz. Tverd. Tela (Leningrad) **17**, 1617 (1975) [Sov. Phys. Solid State **17**, 1057 (1975)].
[15]V. G. Vaks, V. I. Zinenko, and V. E. Shneĭder, Usp. Fiz. Nauk **141**, 629 (1983) [Sov. Phys. Usp. **26**, 1059 (1983)].
[16]W. A. Oates, J. Less Common Met. **88**, 411 (1982).
[17]C. Demangeat, M. A. Khan, G. Moraitis, and J. C. Parlebas, J. Phys. (Paris) **41**, 1001 (1980); J. Khalifeh, G. Moraitis, M. A. Khan, and C. Demangeat, Preprint, Université L. Pasteur, Strasbourg, France, 1983.
[18]F. Perrot and M. Rasolt, Phys. Rev. **B27**, 3273 (1983).
[19]A. C. Switendick, in: Hydrogen in Metals (eds. G. Alefeld and J. Völkl), Vol. 1, Ch. 5 (Russ. transl. Mir, Moscow, 1980).
[20]L. D. Landau and E. M. Lifshitz, Statisticheskaya fizika, Ch. 1, Nauka, Moscow (1976) (Statistical Physics, Pergamon, New York).
[21]J. D. Bernal, Proc. R. Soc. London **A280**, 299 (1964).
[22]J. A. Barker and D. Henderson, Rev. Mod. Phys. **48**, 587 (1976).
[23]A. G. Khachaturyan, Teoriya fazovykh prevrashcheniĭ i struktura tverdykh rastvorov (Theory of Phase Transitions and Structure of Solid Solutions), Nauka, Moscow, 1974.
[24]B. M. Powell, P. Martel, and A. D. B. Woods, Can. J. Phys. **55**, 1601 (1977).
[25]R. I. Sharp. J. Phys. C **2**, 421 (1969).
[26]A. M. Bratkovsky, V. G. Vaks, S. P. Kravchuk, and A. V. Trefilov, J. Phys. **F12**, 1293 (1982).
[27]D. J. W. Geldart and R. Taylor, Can. J. Phys. **48** 167 (1970).
[28]P. Vashishta and K. S. Singwi, Phys. Rev. **B6**, 855, 4883 (1972).
[29]D. J. W. Geldart and S. H. Vosko, Can. J. Phys. **44**, 2137 (1966).
[30]H. Metzger, H. Behr, G. Steyrer, and J. Peisl, Phys. Rev. Lett. **50**, 843 (1983); H. Behr, H. M. Keppler, G. Steyrer, *et al.*, J. Phys. F **13**, L29 (1983).
[31]V. G. Vaks and A. I. Larkin, Zh. Eksp. Teor. Fiz. **49**, 975 (1965) [Sov. Phys. JETP **22**, 678 (1966)].

Translated by Dave Parsons